„BABEŞ-BOLYAI" UNIVERSITY

FACULTY OF PHYSICS

Department of Biomedical Physics

PhD Thesis Summary

STUDY OF SOME BIOMATERIALS FOR CANCER THERAPY AND BONE RECONSTRUCTION

Scientific supervisor:

Prof. dr. Viorica Simon

PhD student

Monica Tămăşan

Cluj–Napoca 2010

Cuprins

1. INTRODUCTION

In the last decades multiple strategies of non-invasive treatment of the malignant tumors were developed, like *radiotherapy* or *chemotherapy*. But these therapies haven't allways expected results and often presents secondary effects. In order to avoid these problems were conceived treatments that attend only the distruction of the cancer cells, by injecting intravenously into the artery that provides blood to the diseased organ, of some specific biomaterials called *radioactive microspheres*. An advantage of this system is that it emits a localized form of beta radiation that minimizes damage to nearby healthy tissue[1]. Rare-earth aluminosilicate glasses permit malignant tumors to be irradiated inside the body at much higher levels than would be possible externally.

Hyperthermia is a type of cancer treatment in which body tissue is exposed to high temperatures (up to 41-47°C). Research has shown that high temperatures can damage and kill cancer cells, usually with minimal injury to normal tissues[2]. By killing cancer cells and damaging proteins and structures within cells[3], hyperthermia may shrink tumors. Numerous clinical trials have studied hyperthermia in combination with radiation therapy and/or chemotherapy.

The purpose of the first part of this study is synthesis and thermal and structural analyses by sol-gel method of some rare-earth aluminosilicate vitroceramics proper for combined therapies of internal radiotherapy and hyperthermia.

By sol-gel method can be obtained materials of high purity and omogenity at much lower temperatures than those used in classical ways of obtaining vitroceramics (melting). Considering the complexity of the sol-gel method were prepared many sistems following the optimisation of the preparing parameters such as: variation of the concentration of Fe and radioactivable elements with silicon concentration, two different precursors for silicon (silicic acid – anorganic and TEOS – organic), as well as two ways to obtain the hydrolysis în the sol-gel process, acid and basic ways.

Another class of materials studied also for cancer treatment applications are phyllosilicate clays as transport platforms and excipients in new chemotherapeutic systems. Clay minerals from phyllosilicate group (palygorskite, sepiolite, kaolinite, talc, montmorillonite, saponite and hectorite) are used from ages in medical and cosmetic purposes.[4,5]

---

1 White J. E., Day D. E., Rare earth aluminosilicate glasses for in vivo radiation delivery, *Key Engineering Materials*, 181, 94-95, 1994.

2 van der Zee J. Heating the patient: A promising approach? *Annals of Oncology* , 13, 1173–1184, 2002.

3 Hildebrandt B., Wust P., Ahlers O. *et al*., The cellular and molecular basis of hyperthermia, *Critical Reviews in Oncology/Hematology*, 43, 33–56, 2002.

4 Carretero, M.I., Pozo, M., Clay and non-clay minerals in the pharmaceutical industry Part I. Excipients and medical applications., *Appl. Clay Sci*. 46, 73–80, 2009.

Chemotherapy is one of the primary methods of treatment of cancer. It uses chemical agents to kill the cancer cells. Unfortunately, tumor cells respond only moderately to the current standard chemotherapy. The underlying reason for this insensitivity to the chemotherapy is that cancer cells have many defense mechanisms to resist the drug actions. They can reduce cell drug concentration by slowing the drug's entry into the cells, ejecting drugs out of the cells with specialized pumps, and by converting drugs into harmless forms. Current therapeutic regiments, however, can only slowly deliver a low concentration of drugs to cancer cells in a discontinuous manner. As a result, the drug concentration in cancer cells is too low to effectively kill them. More importantly, the cancer cells surviving this low drug concentration are induced to become even more drug-insensitive, causing treatment failure. Chemotherapy acts by killing cells that divide rapidly, one of the main properties of cancer cells. This means that it also harms cells that divide rapidly under normal circumstances: cells in the bone marrow, digestive tract and hair follicles; this results in the most common side-effects of chemotherapy–myelosuppression (decreased production of blood cells), mucositis (inflammation of the lining of the digestive tract) and alopecia (hair loss).

Nanoparticles have been demonstrated to be able to preferentially deliver drugs to diseased tissues resulting in enhanced therapeutic efficacy. Nanoparticles (NPs) of biodegradable polymers as a drug delivery system realize controlled drug release and achieve better therapeutic efficacy than pristine agent. However, the low selectivity of NPs towards cancer cells hinders the advantages of NP formulation for efficient chemotherapy. Novel systems of chemoterapeutic agents loaded in montmorillonite (PLGA /MMT) NPs for targeted drug delivery were developed. **As a potent detoxifier, the medical clay MMT can adsorb toxins and reduce side effects**. The drug delivery system represents a new concept in developing drug delivery systems and can achieve functions such as to formulate anticancer drugs with no harmful adjuvant, to reduce side effects caused by formulated drugs and to have synergistic therapeutic effects.[6]

It is a new direction that anticancer drugs can be formulated in nanoparticles of another drug, which functions as matrix material or a component of the matrix material of the nanoparticles and may have therapeutic effects for the side effects of the encapsulated drug. One suitable class of chemicals for use as the first drug used as the matrix or carrier is the class of medical clays. One of the clays already tested as a component of NPs is montmorillonite (MMT)/poly(D,L-lactide-co-glycolide) (PLGA) nanoparticles. The idea is to make use of the mucoadhesive property and therapeutic effects of medical clays such as MMT to make a novel

---

[5] Carretero, M.I., Pozo, M., Clay and non-clay minerals in the pharmaceutical industry Part II. Active ingredients., *Appl. Clay Sci.* 47, 171–181, 2010.

[6] Bingfeng S., Balu R., Si-Shen F., Multifunctional poly(D,L-lactide-co-glycolide) /montmorillonite (PLGA/MMT) nanoparticles decorated by Trastuzumab for targeted chemotherapy of breast cancer, *Biomaterials* **29**, 475, 2008.

kind of nanoparticle to delivery drugs such as anticancer drugs across a mucosal membrane such as the gastrointestinal (GI) barrier to realize administration of the second drug.

A medical clay used for a large range of disfunctions as well as for the detoxifying of the organism was considered for a matrix material in a targeted delivery drug and investigated by X-ray diffraction analysis, thermal analyses DTA/TG and DSC, specific surface area using nitrogen adsorption/desorption method and Scanning Electron Microscopy with Elemental microanalysis by X-ray Diffraction (SEM/EDX). Influence of two thermal tratments (at 700ºC and 1000ºC) on structure and morphology of the sample and influence of acid or basic environnement on specific surface area and porosimetry were also conducted. Other three types of commercial clays (FARM, FAV and RN), were analysed by thermal and structural methods. Specific surface analyses and porosimetry measurements were also made on the samples immersed for one week in acid and in basic medium.

The third part of the studies rely on a batch of bone materials having animal and human origins (deproteinate animal and human bones, and deer antler) with applications in developing biomaterials for bone reconstructions. Materials were analysed by X-ray diffraction analysis, thermal analyses DTA/TG, DSC and Scanning Electron Microscopy. Moreover, a kinetic study for calculating activation energies of decomposition reactions by thermal energy was made for deer antler of different ages sterillized by γ irradiation.

The thesis is structured in 11 chapters. First 5 chapters contain informations from literature concerning studied materials: ***Biomaterials developed in last decades for cancer therapies*** (*Radioactive microspheres used in brachitherapy, Magnetic nanostructured materials used in hyperthermia treatment of cancer, Medical clays used as transport platforms in cancer treatment by chemotherapy*), and ***Biomaterials for bone reconstruction***. Chapter 6 presents theoretical description of analyses methods (thermal analyses, structural by X-ray Diffraction, Scanning Electron Microscopy, specific surface area and pore volume and area by BET method). Chapters 7-8-9 presents experimental results on each three types of studied materials: Chap. 7 – Experimental results for vitroceramic materials for cancer therapy; Chap. 8 – Experimental results for clay minerals; Chap. 9 – Experimental results for materials for bone reconstruction. Chapter 10 include selected conclusions for the three sets of experimental results, while Chapter 11 contains bibliografic references in alphabetical order.

Keywords: rare-earth aluminosilicate glasses, sol-gel method, brachitherapy, hyperthermia, phyllosilicates, thermal analyses, X-ray Diffraction, specific surface area, porosimetry, BET method, kinetic analysis, deer antler, hydroxiapatite, bone reconstruction

2. VITROCERAMIC MATERIALS FOR CANCER THERAPY

2.1 Preparing aluminosilicates by sol-gel method

Precursors for SiO_2, were $C_8H_{20}O_4Si$ (tethraethylorthosilicate, TEOS) and $SiO_2 \cdot xH_2O$ (silicic acid), and precursor for Al_2O_3 was $Al(NO_3)_3 \cdot 9H_2O$. In order to include Fe and radioactivable elements were used their nitrates, namely $Fe(NO_3)_3 \cdot 9H_2O$, $Y(NO_3)_3 \cdot 6H_2O$ and respectively $Dy(NO_3)_3 \cdot 5H_2O$. Acid hydrolisis (pH 1.5) was achieved by adding a few drops of azotic acid (HNO_3), and basic hydrolisis (pH 8.5) was obtained by adding a few drops of ammonium hydroxid (NH_4OH).

The pH effect in sol-gel process was studied first on two samples from silicic acid as precursor, having the composition **$66.66\ SiO_2$ x $33.33\ Al_2O_3$**, one by acid hydrolisis (pH 1.5) and the other by basic hydrolisis (pH 8.5); the samples were labelled S(1.5) and S(8.5).

Systems prepared from TEOS as precursor of SiO_2, with basic pH (8.5) were:

- **$(100\text{-}x)[SiO_2] \cdot 20Al_2O_3 \cdot x[Fe_2O_3]$, with x = 0, 5, 10, 15 şi 20% mol.**

Systems prepared from silicic acid ($SiO_2 \cdot xH_2O$) as precursor of SiO_2, were:

- **$(100\text{-}x)[SiO_2] \cdot 20Al_2O_3 \cdot x[Fe_2O_3]$, with x = 0, 5, 10, 15 şi 20% mol.**

These systems were prepared at acid pH (1.5) and basic pH (8.5) as well.

Systems with radioactivable elements prepared and analyzed are:

- **$75\ SiO_2 \cdot 20\ Al_2O_3 \cdot 5\ Y_2O_3$ and $75\ SiO_2 \cdot 20\ Al_2O_3 \cdot 5\ Dy_2O_3$**

2.2 Characterisation of aluminosilicate samples by thermal analyses

Thermal differential and thermogravimetry were made on a derivatograf Shimadzu type *DTG-60/60H*. Calorimetric analyses were conducted on a differential calorimeter Shimadzu type ***DSC-60***.

Calorimetric and thermogravimetric analyses revealed a thermal behavior similar for the samples from TEOS as precursor and for those synthesized by basic pH. All these samples presents four endothermic peaks at the same temperatures ad these peaks were correlated with specific thermal events:

– Two endothermal peaks with maximum at ~50ºC and at 100ºC respectively, associated with a mass loss in TG, were identified as a dehydration of water from the surface of the materials, and with the elimination of the water resulted from the reaction of the ammonium hydroxid (NH_4OH) with azotic acid HNO_3, resulted from the precursor used for Al [$Al(NO_3)_3 \cdot 9H_2O$]:

$$NH_4OH + HNO_3 \rightarrow NH_4NO_3 + H_2O$$

– At 130ºC and at 172ºC two endothermic events well defined, with no mass loss in TG. The peak with maximum at 130ºC (T_{onset} = 127ºC) correspons to a structural transformation of the ammonium nitrate resulted from the above mentioned reaction, transformation which, acording to literature, apears at T = 125.2ºC[7] . The event at 172ºC (T_{onset} = 169ºC) is associated with the melting of the ammonium nitrate.

– A large endothermal event with maximum ta ~230 ºC accompanied with a mass los quite large (~44–50%). Characteristics of this curve indicate an overlay effect of several processes, among which are the decomposition of the ammonium nitrate, begining at T~220ºC, according to the reaction

$$NH_4NO_3 \rightarrow N_2O + 2H_2O \rightarrow N_2 + 1/2\ O_2 + 2H_2O$$

and the elimination of the evolved products, and also the decomposition of the organic monomers left in the matrix from TEOS precursor.

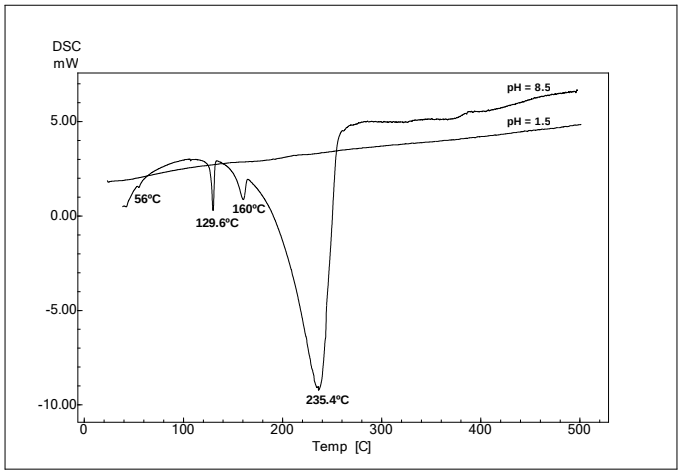

DSC analyses for $66.66SiO_2 \cdot 33.33Al_2O_3$ from silicic acid

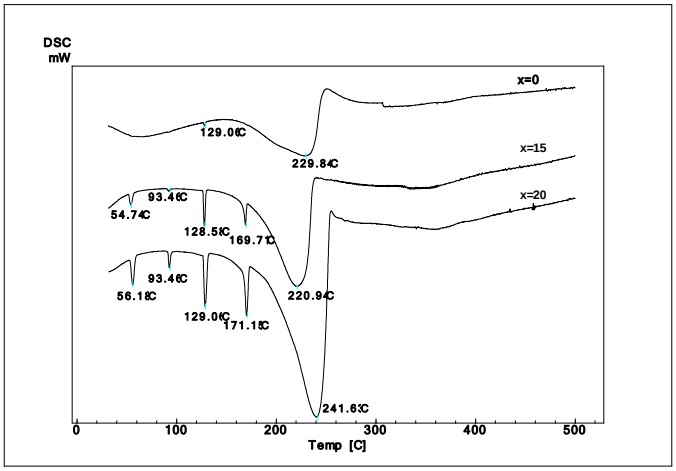

*DSC analyses for **$(100-x)[SiO_2] \cdot 20Al_2O_3 \cdot x[Fe_2O_3]$** with x = 0, 15, 20, from TEOS, pH 8.5.*

[7] Brown R. N., McLaren A. C., On the Mechanism of the Thermal Transformations in Solid Ammonium Nitrate, *Proceedings of the Royal Society of London. Series A, Mathematical and Physical Sciences*, 266, 1326, 329-343, 1962.

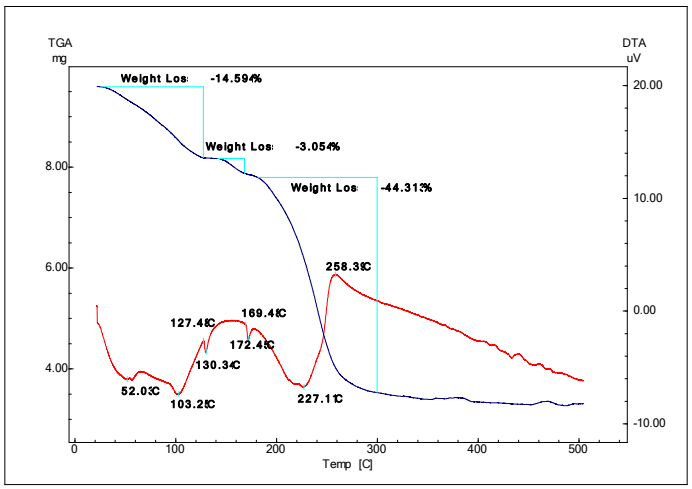

DTA/TG analyses for $80SiO_2{\cdot}20Al_2O_3$ from TEOS, pH 8.5

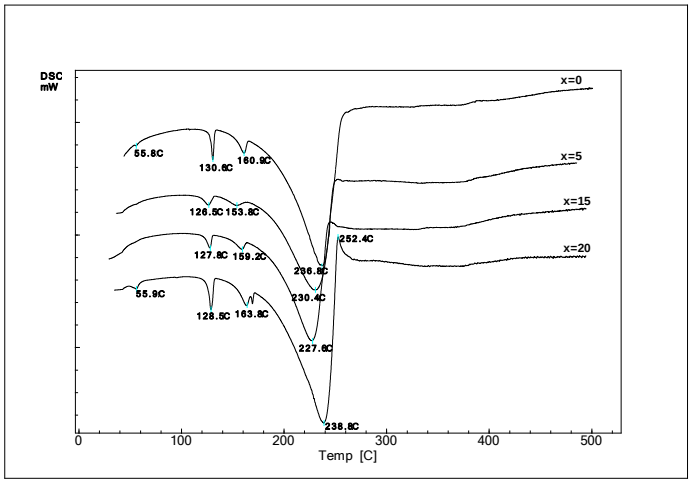

DSC analyses for ***(100-x)[SiO_2]· 20Al_2O_3· x[Fe_2O_3]****, with x = 0, 5, 15, 20, from silicic acid, pH 8.5*

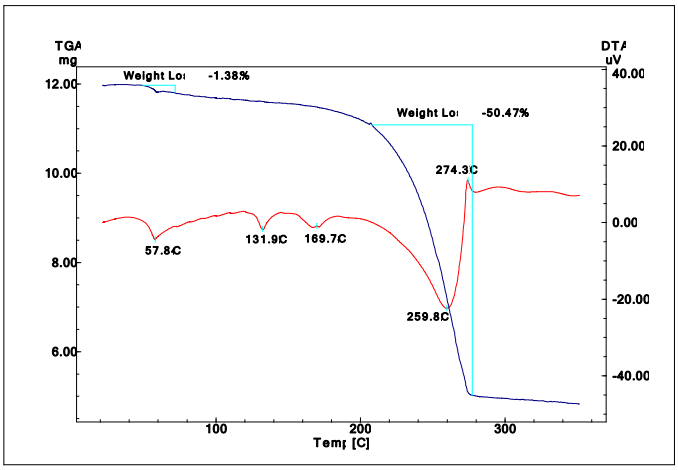

DTA/TG analysis for $60SiO_2{\cdot}20Al_2O_3{\cdot}20Fe_2O_3$ from silicic acid, pH 8.5.

Samples from silicic acid and those synthesized with acid pH (1.5) present only thermal events characteristic to the water and nitrates losses:

– at T_{max} ~ 100ºC an endothermic peak accompanied in TG by a mass loss can be associated with the elimination of the water at the surface of the material;
– at T_{max} ~ 200ºC a very small endothermic peak accompanied by a mass loss of ~5.4%, which can be the result of the decomposition of the nitrates from Al_2O_3 precursor.

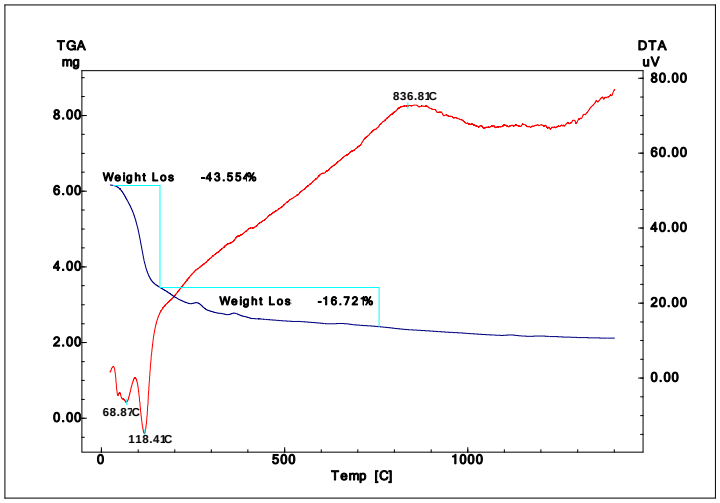

DTA/TG analysis for S-75SiO_2·20Al_2O_3·5Fe_2O_3 from acid silicic, pH 1.5

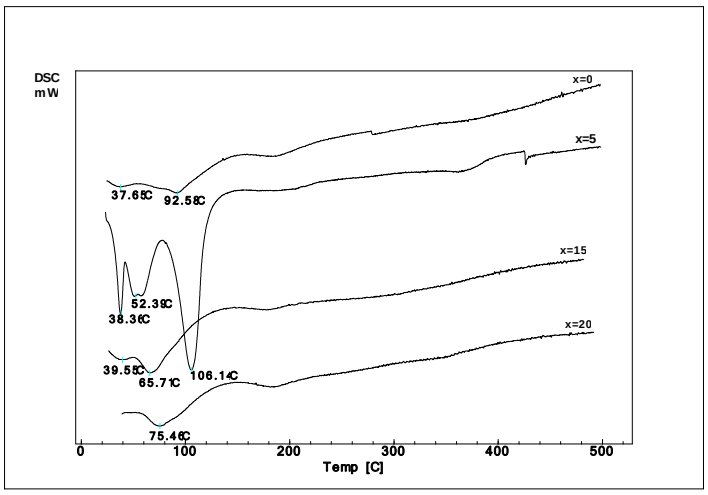

DSC analyses for ***(100-x)[SiO_2]· 20Al_2O_3· x[Fe_2O_3]*** samples, *with x = 0, 5, 15, 20, from silicic acid, pH 1.5*

The DSC recordings for the samples from silicic acid as precursor indicate a better thermal stability than those from TEOS as precursor, after the temperature of 200ºC there are no more thermal events, while the endothermic peaks bellow 100ºC can be associated with dehydration processes and of decomposition processes with removal ot the nitrates from Al and Fe precursors.

The systems containing radioactivable elements –Yttrium and Dysprosium – were obtained by adding nitrates precursors [$Y(NO_3)_3·6H_2O$ şi resp. $Dy(NO_3)_3·5H_2O$], dissolvated in distilled water. Silicon precursor was silicic acid. Thermal analyses DTA/TG were conducted

on systems containing 5% of radioactivable element: **$75SiO_2 \cdot 20Al_2O_3 \cdot 5Y_2O_3$** and **$75SiO_2 \cdot 20Al_2O_3 \cdot 5Dy_2O_3$**.

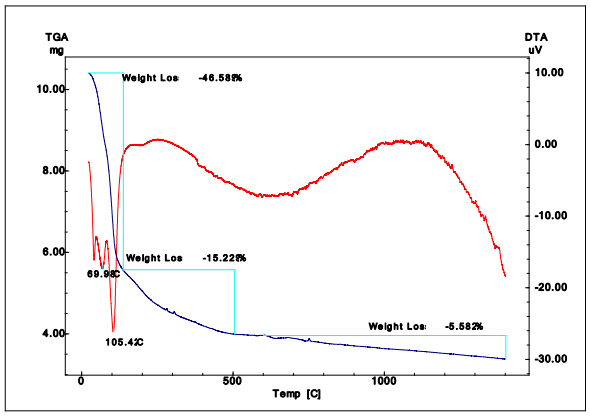

DTA/TG analysis for $75SiO_2 \cdot 20Al_2O_3 \cdot 5Y_2O_3$

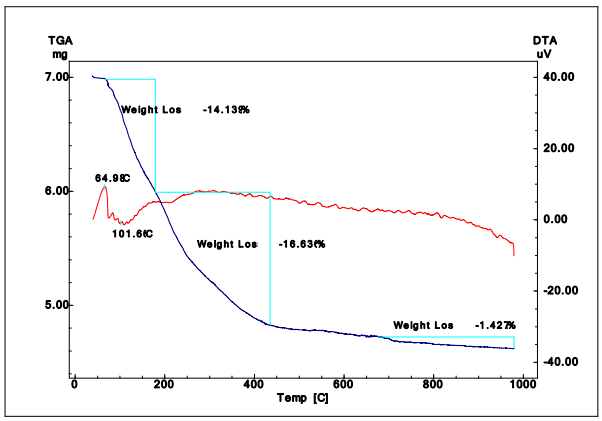

DTA/TG analysis for $75SiO_2 \cdot 20Al_2O_3 \cdot 5Dy_2O_3$

These results lead us to the observation that, after the preparation, in the matrix of the as prepared systems remain important amounts of organic nature (for the samples from TEOS) and anorganic nature (nitrates) and these residues have to be eliminated through thermal treatments. Thermal analyses evidenced that the mass losses take place up to 500ºC, where, in some cases, begins the developing of the first crystallization grains. To evaluate the structural evolution of the materials and of the crystalline phases nedeed for the practical applications of these systems two thermal treatments were made at temperatures of 500ºC for 30 minutes and at 1200ºC for 24h.

2.3 Structural characterization of the samples by XRD

Structural studies were conducted on Shimadzu XRD-6000 difractometer. Aquisitioning parameters were: operating tension 40 kV, current 30 mA. Measurements were made at speed of 2º/min, step of 0.02 on a scanning domain 2θ of 10-100º.

Diffractograms of the samples $80SiO_2 \cdot 20Al_2O_3$ prepared from silicic acid and from TEOS indicate an amorphous structure for both systems.

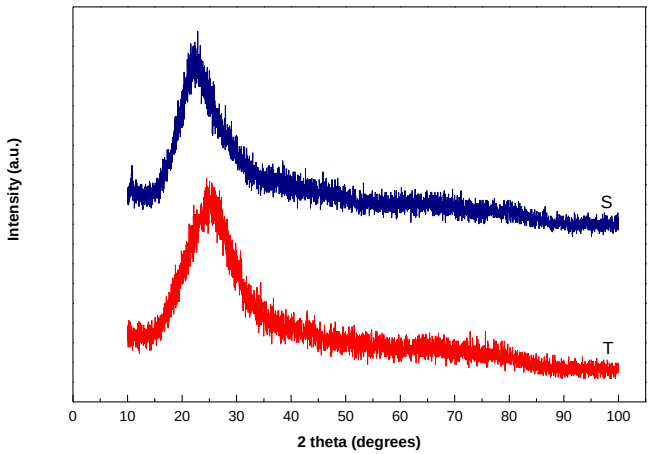

Diffractograms of $80SiO_2{\cdot}20Al_2O_3$ from silicic acid (S) and TEOS (T)

XRD analyses of aluminosilicates with 5, 15 and 20% Fe prepared from silicic acid with acid pH and bazic respectively, before and after thermal treatments:

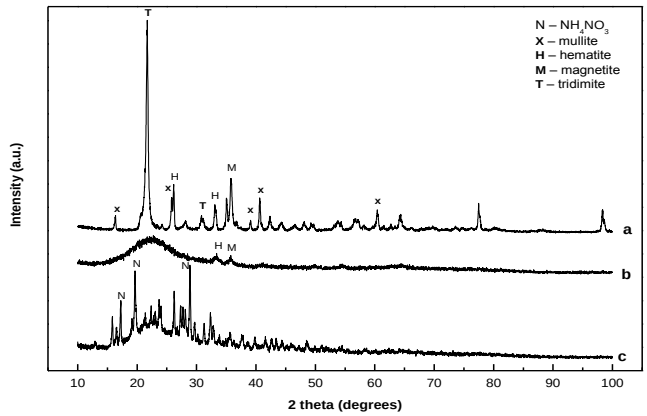

Difractograms of samples $75SiO_2 \cdot 20Al_2O_3 \cdot 5Fe_2O_3$ from silicic acid at pH 1.5, before (c) and after thermal treatments from 500ºC (b) and 1200ºC (a).

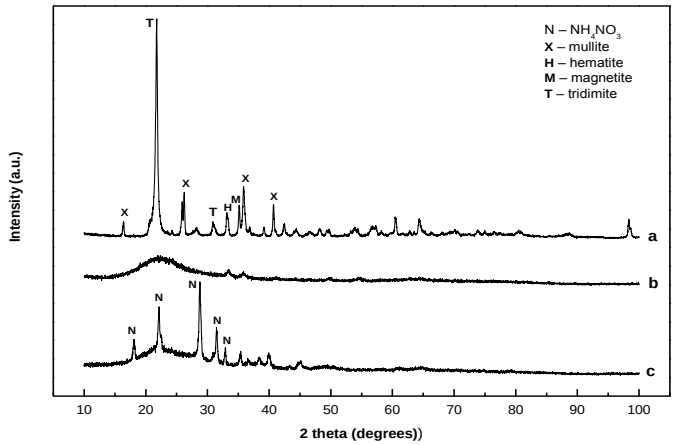

Difractograms of samples $75SiO_2 \cdot 20Al_2O_3 \cdot 5Fe_2O_3$ from silicic acid at pH 8.5, before (c) and after thermal treatments at 500ºC(b) and 1200ºC(a).

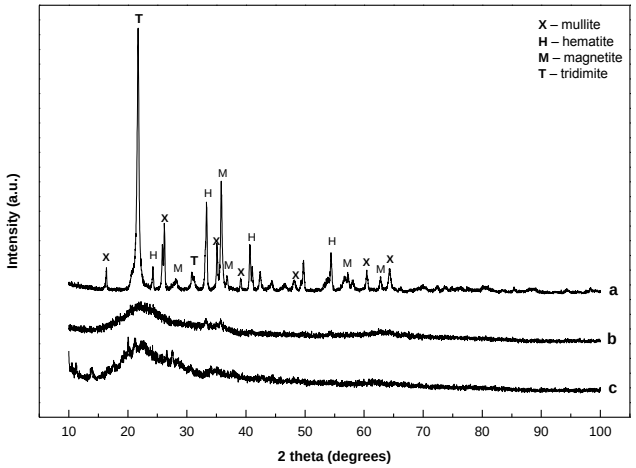

Difractograms of samples $65SiO_2 \cdot 20Al_2O_3 \cdot 15Fe_2O_3$ from silicic acid at pH 1.5, before (c) and after thermal treatments at 500ºC(b) and 1200ºC(a)

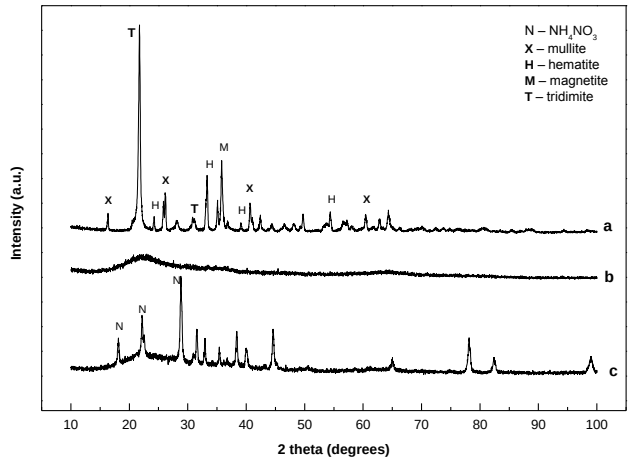

Difractograms of samples $65SiO_2 \cdot 20Al_2O_3 \cdot 15Fe_2O_3$ from silicic acid at pH 8.5, before (c) and after thermal treatments at 500ºC(b) and 1200ºC(a)

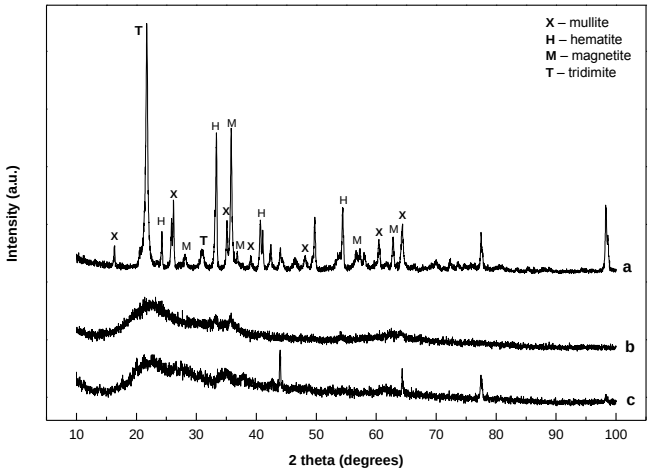

Difractograms of samples $60SiO_2 \cdot 20Al_2O_3 \cdot 20Fe_2O_3$ from silicic acid at pH 1.5, before (c) and after thermal treatments at 500ºC(b) and 1200ºC(a)

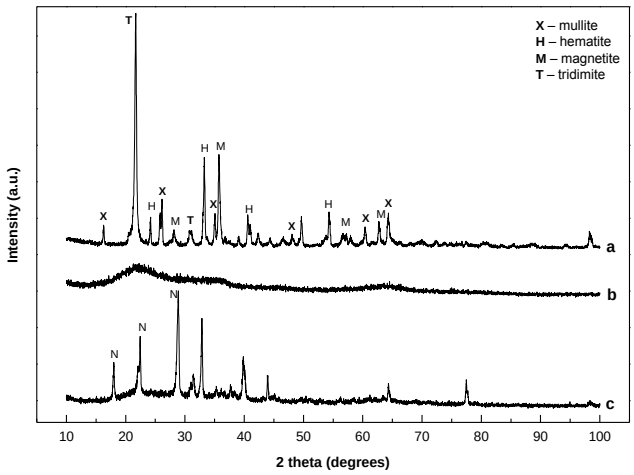

Difractograms of samples $60SiO_2 \cdot 20Al_2O_3 \cdot 20Fe_2O_3$ from silicic acid at pH 8.5, before (c) and after thermal treatments at 500ºC(b) and 1200ºC(a)

After the thermal treatment at 500ºC the structure of the samples remains mostly amorphous, diffractograms present only two small peaks indicating the formation of the first crystallization grains of the hematite and magnetite phases, while after the termal treatment at 1200ºC the samples reveal a major crystalline structure. Four crystalline phases were identified: hematite (Fe_2O_3), magnetite (Fe_3O_4), mullite ($Al_6Si_2O_{13}$) and tridimite (SiO_2). Mean dimensions of the crystallites, calculated on the basis of the Scherrer equation, are presented in *Table 1*.

Table 1. *Mean dimensions of the crystallites in the systems* ***$(100\text{-}x)[SiO_2]\cdot 20Al_2O_3\cdot x[Fe_2O_3]$****, x = 5, 15 and 20 from silicic acid, pH 1.5 and 8.5 after termal tratments at 500ºC and 1200ºC.*

Sample	**Treatment temperature**	**tridimite** (SiO_2) [nm]	**mullite** ($Al_6Si_2O_{13}$) [nm]	**hematite** (Fe_2O_3) [nm]	**magnetite** (Fe_3O_4) [nm]
$75SiO_2\cdot 20Al_2O_3\cdot 5Fe_2O_3$	tt 500ºC	–	–	10.41	12.54
(pH 1.5)	tt 1200ºC	21.82	36.68	20.81	23.04
$75SiO_2\cdot 20Al_2O_3\cdot 5Fe_2O_3$	tt 500ºC	–	–	12.56	11.70
(pH 8.5)	tt 1200ºC	23.08	32.12	22.29	24.48
$65SiO_2\cdot 20Al_2O_3\cdot 15Fe_2O_3$	tt 500ºC	–	–	13.91	9.20
(pH 1.5)	tt 1200ºC	23.59	36.79	28.38	32.01
$65SiO_2\cdot 20Al_2O_3\cdot 15Fe_2O_3$	tt 500ºC	–	–	12.56	11.70
(pH 8.5)	tt 1200ºC	25.13	35.81	26.29	29.86
$60SiO_2\cdot 20Al_2O_3\cdot 20Fe_2O_3$	tt 500ºC	–	–	13.77	10.82
(pH 1.5)	tt 1200ºC	22.95	36.54	30.54	31.42
$60SiO_2\cdot 20Al_2O_3\cdot 20Fe_2O_3$	tt 500ºC	–	–	–	–
(pH 8.5)	tt 1200ºC	25.42	33.79	34.26	30.51

The diffractograms of the untreated samples evidenced an amorphous structure with only one crystalline phase of NH_4NO_3 (nitrammite), a phase that disappears after the thermal treatment at 500ºC, when first grains of hematite and magnetite evolve in dimensions of 9-15 nm; after the thermal treatment at 1200ºC the dimensions of these crystallites are up to 35 nm. Other crystalline phases identified in samples treated at 1200ºC are tridimite (SiO_2) and mullite ($Al_6Si_2O_{13}$), with dimensions between 20-40 nm.

From thermal and structural analyses one can conclude that regardless the preparation parameters involved (SiO_2 precursor, pH), after the thermal treatments the samples presents a polycrystalline structure with hematite and magnetite phases, which are to be implied in cancer treatment by hyperthermia applications. Furthermore, a growingly Fe concentration in the structure generate crystallites with greater dimensions after thermal treatment at 1200ºC. The samples from basic pH evolves hematite crystallites with dimensions greater that those from acid pH, while the dimension of the magnetite crystallites is about the same. Another observation would be that, regardless the pH, for the same Fe concentration, the magnetite crystallites are a bit larger (with few nm) than those oh hematite.

3. EXPERIMENTAL RESULTS OF MINERAL CLAYS

3.1 Structural analyses by X-ray diffraction

Diffractogram of ALGO sample indicate a major crystalline phase – *kaolinite* [$Al_2Si_2O_5(OH)_4$]. Kaolinite is a silicatic mineral structurated from tethraedal silicon sheets crosslinked through oxigen atoms by other sheet of aluminum octhaedra.

X-ray diffractogram of FAV sample presents peaks corresponding crystalline phases of *illlite* [$K_{0.7}Al_{12}(Si,Al)_{40}O_{10}$] and *quartz* SiO_2. In the FARM sample were identified crystalline phases of: *quartz* (SiO_2) and *kaolinit-montmorillonite* [$Na_{0.3}Al_4Si_6O_{15}(OH)_6$]. In X-ray diffractogram of RN sample were identified crystalline phase of *illite* $(K,H_3O)(Al,Mg,Fe)_2(Si,Al)_4O_{10}[(OH)_2,(H_2O)$ –and *quartz* SiO_2.

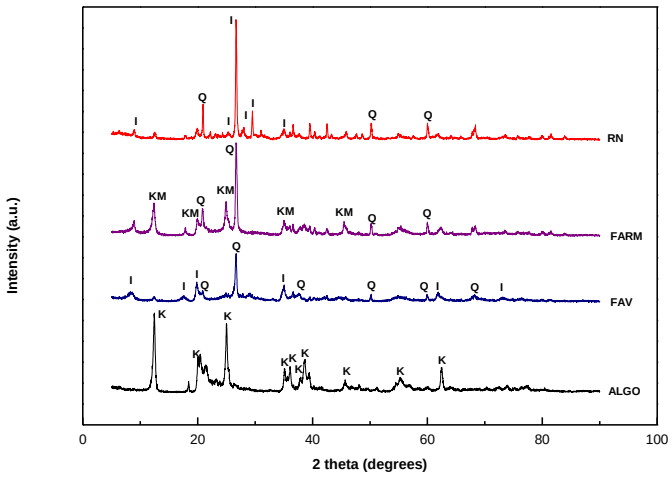

X-ray diffractograms of the clay mineral samples (K–kaolinite, Q–quartz, I–illiet, KM–kaolinite-montmorillonite)

3.2 Thermal analyses of mineral clays

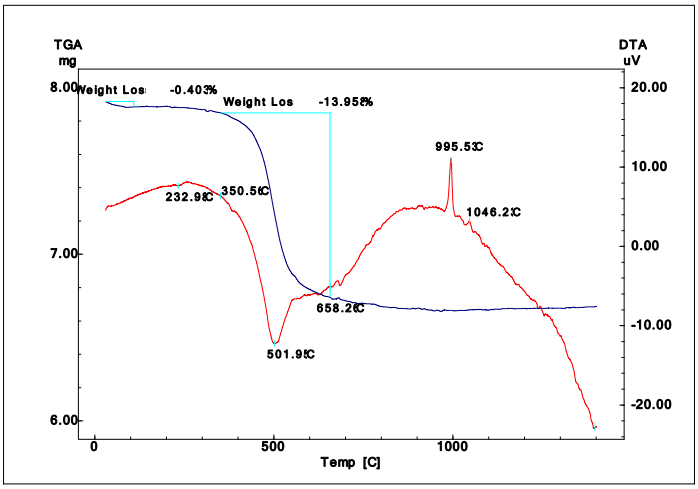

DTA/TG analysis of ALGO sample

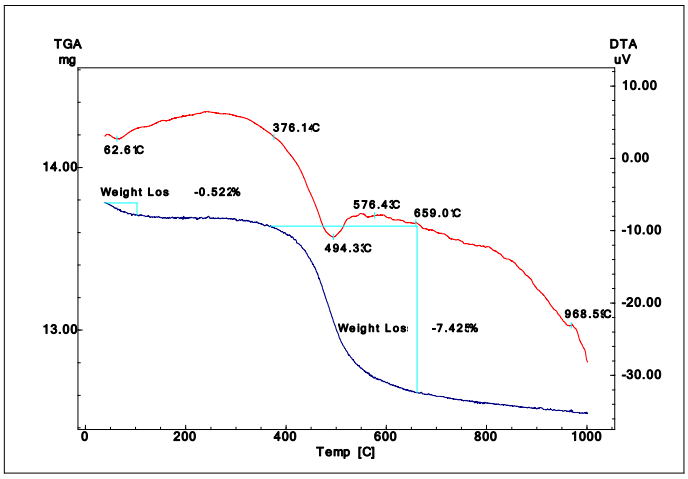

DTA/TG analysis of FARM sample

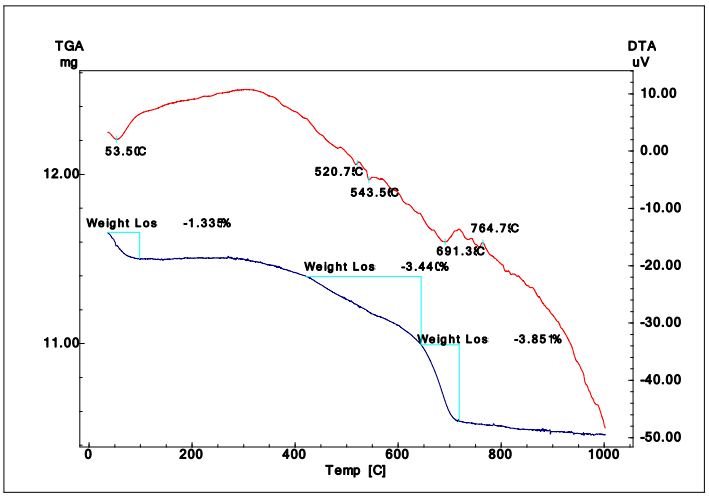

DTA/TG analysis of RN sample

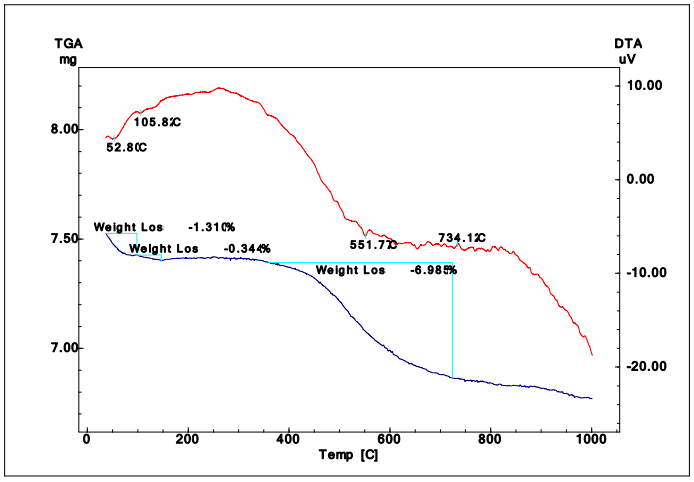

DTA/TG analysis of FAV sample

Thermal analyses confirmed X-ray diffraction results, the shapes of the thermic and thermogravimetric recordings match the crystalline phases identified. Thermic events characteristic to mineral clays revealed by the DTA/TG signals were *dehydration*, *dehydroxilation* (having maximum temperatures and temperature ranges different for each type of mineral clay) and *a structural transformation* at high temperatures (above 900ºC).

3.2 Influence of the thermal treatmens on the structure of the mineral clays and influence of the immersion environement on the surface and porosimetry characteristics

ALGO sample was calcinated for a period of 30 min, at 700ºC and 1000ºC, after that samples were analyzed by X-ray diffraction and Scanning Electron Microscopy and elemental microanalysis by Energy Dispersive X-ray spectroscopy.

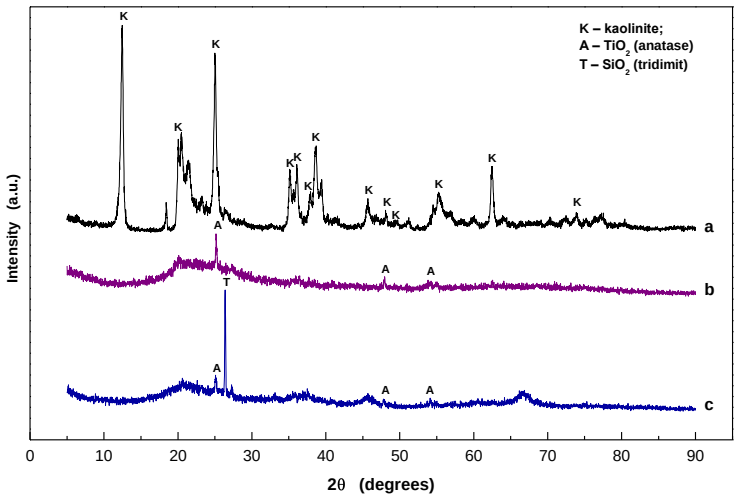

Diffractograms of ALGO sample before (a) and after heat treatments at 700ºC (b) and 1000ºC (c).

The structure of the ALGO samples calcinated at 700 and 1000 ^{o}C reveals the disruption of the ordered structure based on hydroxil bonds of the mineral clay. Crystalline phases identified in the raw sample (*a*) disappear after calcination. Diffractogram of the sample calcinated at 700ºC for 30 min (*b*) presents only a few peaks correspondent to the crystalline phase of anatase, TiO_2. In the sample treated at 1000ºC for 30 min (*c*) SiO_2 peaks are identified (in the polymorphous form of tridimite) and small anatase peaks.

Scanning Electron Microscopy and elemental microanalysis by Energy Dispersive X-ray spectroscopy (SEM/EDX) were involved to explore the morphology and elemental composition of the ALGO sample before and after calcination. Analyses were conducted on a Jeol JSM 5510LV microscope. Images are at a magnification scale of de 1 µm (50µm in the inset image).

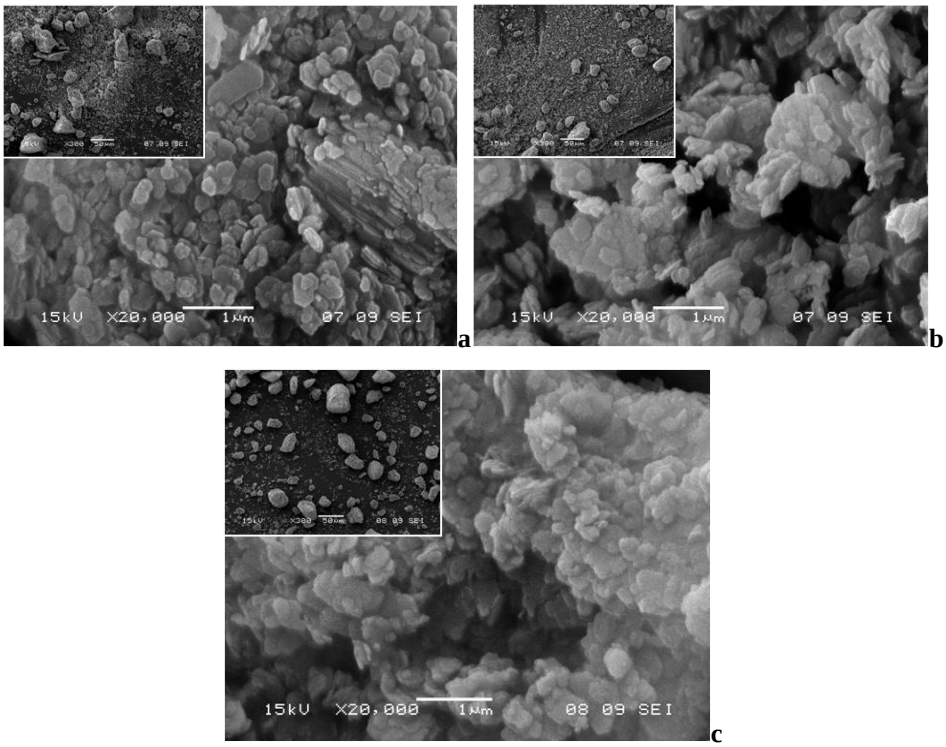

SEM images of ALGO (a – untreated; b –thermal treatment at 700ºC; c – thermal treatment at 1000ºC).

Morphology of the untreated sample (*fig. a*) shows a well crystallized structure characterized by hexagonal and pseudohexagonal layered crystallites, a kaolinite type texture[8]. The treated sample (*Fig. b* and c) present a more compacted structure with rounded edges; in the sample treated at 700ºC large pores and solid blocks can be observed, while the sample treated at 1000ºC is less porous and more compacted. Elemental composition of the untreated sample, determinated by SEM/EDX microanalysis is indicated in *Table 2*. Additional elements to those from kaolinite structure, *i.e.* Al, Si and O, were found N, C and Ti.

[8] Zbik M., Smart R. St.C., Nanomorphology of kaolinites: comparative SEM and AFM studies, *Clay Clay Miner*. 46, 153-160, 1998.

Table 2 *Elemental composition of ALGO sample from SEM/EDX analysis.*

Chemical element	O	N	C	Ti	Si	Al
Relative concentration (%)	53.61	2.97	15.89	2.00	13.15	12.38

Textural properties characterisation of ALGO sample, untreated and treated at 700ºC as well as 1000ºC, by specific surface area and porosimetry measurements was conducted on a Sorptomatic 1990 Analyzer, working on the principles of Brunauer, Emmet and Teller (BET) theory for multlayed adsorbtion/desorbtion of gas molecules on solids[9].

The shape of adsorbtion/desorbtion isotherms is characteristic to type IV, specific to mesoporous materials; the untreated and 700ºC heat treated samples present similar isotherms, while the sample 1000ºC heat treated reveal a more concave isotherm, corresponding to smaller values of specific surface area and pore volume.

Table 3*. Specific surface area and pore volumes from BET analyses*

Proba	**ALGO**	**ALGO tt 700ºC**	**ALGO tt 1000ºC**
Specific surface area (BET 3 parameters method) [m^2/g]	28.139	29.451	18.103
Pore volume (Gurvich) [cm^3/g]	0.0756	0.0801	0.0601
Cumulative mesopores volume (BJH) [cm^3/g]	0.0781	0.0983	0.0579
Cumulative micropores volume (HK) [cm^3/g]	0.0145	0.0158	0.0093

Median pore radius calculated from adsorbtion/desorbtion isotherms have values between 0.6÷9.27 nm and indicate micro- and mesopores, according to IUPAC rules.

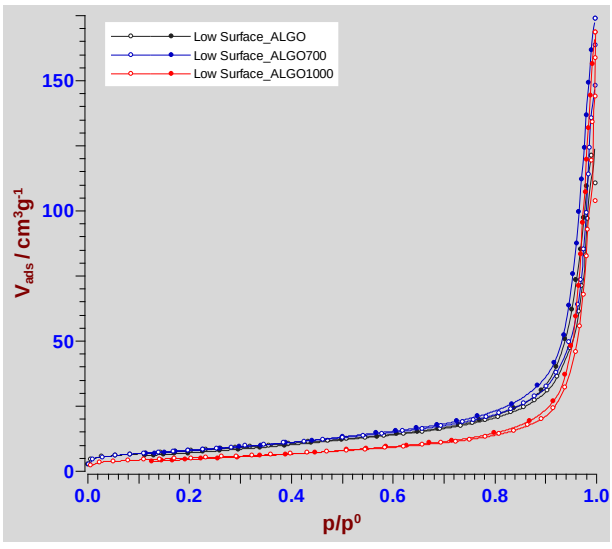

Adsorbtion/desorbtion nitrogen isotherms on ALGO (black – untreated sample; blue –heat treated at 700ºC sample; red – heat treated at 1000ºC sample)

[9] Brunauer S., Emmett P., Teller E., Adsorption of Gases in Multimolecular Layers, *J. Am. Chem. Soc*. 60, 309-319, 1938.

Influence of acid and basic medium, where the medical clay are to be ingested as a step of the treatment process, considering that the gastrointestinal tract present diferent types (value of human saliva pH vary between 5 and 8, acidity of the stomach is 2 and small intestine has a pH around 8[10]), was studied by immersing the 4 clay samples in acid pH (2) and in basic pH (12) solutions for a week. These immersed samples were washed with distilled water and dryed at 35ºC and then analyzed on Sorptomatic 1990 to determine specific surface area and porosimetry. The shape of adsorbtion/desorbtion isotherms remains of type IV. Results obtained from these analyses – specific surface, cumulativ pore volume, meso- and micropores and median pore radius – are presented in *Table 4*.

Table 4. *Textural properties from BET analyses of medical clays imeersed in acid and basic mediums*

				Mesopores (BJH)			Micropores (HK)		
	pH	**Pore volume (Gurvich) [cm^3/g]**	**SSA [m^2/g]**	**Median pore radius [nm]**	**Cumulativ pore volume [cm^3/g]**	**Cumulativ pore area [m^2/g]**	**Median pore radius [nm]**	**Cumulativ pore volume [cm^3/g]**	**Cumulativ pore area [m^2/g]**
ALGO	**2**	0.0716	27.435	9.991	0.0772	25.713	0.4545	0.0145	25.178
	12	0.0717	27.889	9.7664	0.0784	26.743	0.4623	0.0152	27.172
FARM	**2**	0.0634	43.033	4.2602	0.0564	32.893	0.5037	0.0222	36.777
	12	0.067	44.455	5.2991	0.0669	32.917	0.5831	0.0227	31.089
FAV	**2**	0.0572	32.56	4.2724	0.0521	30.227	0.4912	0.0166	27.048
	12	0.0592	38.567	4.1291	0.0497	29.557	0.548	0.0203	33.358
RN	**2**	0.0283	30.497	2.0671	0.0251	19.8	0.407	0.0137	23.283
	12	0.0363	37.284	2.343	0.03	23.274	0.5301	0.0192	30.339

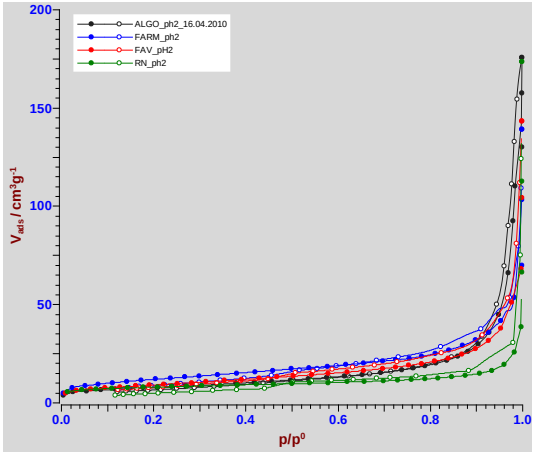

Adsorbtion/desorbtion nitrogen isotherms on ALGO, FARM, FAV and RN immersed in acid medium (pH = 2)

[10] Omen AG, Sips AJ, Groten AM, Dick JP, Sijm TJM, Tolls THM, Mobilization of PCBs and lindane from soil during *in vitro* digestion and their distribution among bile salt micelles and proteins of human digestive fluid and the soil., *Environ. Sci. Technol*. 34, 297-303, 2000.

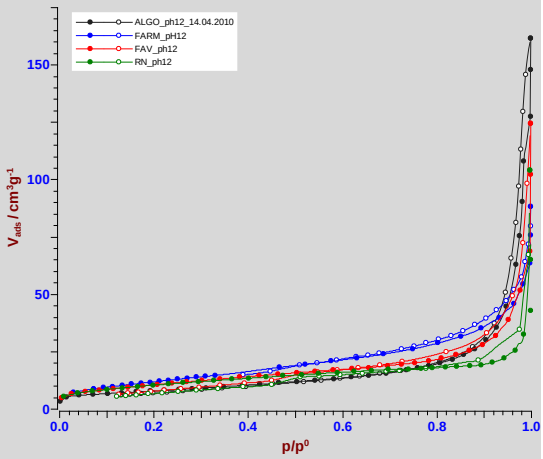

Adsorbtion/desorbtion nitrogen isotherms on ALGO, FARM, FAV and RN immersed in basic medium (pH =12)

The clay samples ALGO, FARM, FAV and RN have a similar behavior after immersion, manifesting an increasing tendincy of the textural properties in basic medium with relatively small values. ALGO sample present a total pore volume larger, but a specific surface area smaller than FARM sample. FAV sample has a specific surface smaller than FARM sample, but larger than ALGO and RN samples, while pore volume is smaller than that of ALGO and FARM samples, and larger than RN sample.

4. EXPERIMENTAL RESULTS OF MATERIALS FOR BONE RECONSTRUCTION

4.1 Materials for bone reconstruction – deer antler, human and animal bones

This study was made in order to obtain materials for bone reconstruction by thermal treatments of certain types of animal bones and deer antler, a bone-like material with remarcable regeneration properties, as well as for distinguishing structural changes and interactions between mineral and organic phases occured with the contribution of thermal energy. Materials analyzed were: human skull bone and animal originated bones (deer antler, pig, cattle, hen, turkey and fish).

4.2 Thermal analyses of bone materials

DTA/TG analyses on bone materials represented in figures bellow highlight a the same thermal behavior on all the samples. DTA signals display two thermal events: one endothermic peak having the maximum temperature in the interval 70-80ºC, accompanied by a mass loss in TG recording (on the interval 50ºC–150ºC), and an large exothermic event in temperature interval 350–500ºC, also accompanied by a considerable mass loss. The first event might

correspond to bone matrix collagen triple helix structure denaturation, event dependent on the hydration degree of the material[11,12,13], but it can correspond also to the elimination of the free water attached on the hydroxyapatite matrix[14,15]. The second event corresponds to the decomposition and combustion of the organic phase of the bone accompanied by the elimination of the gaseous products resulted in the process.

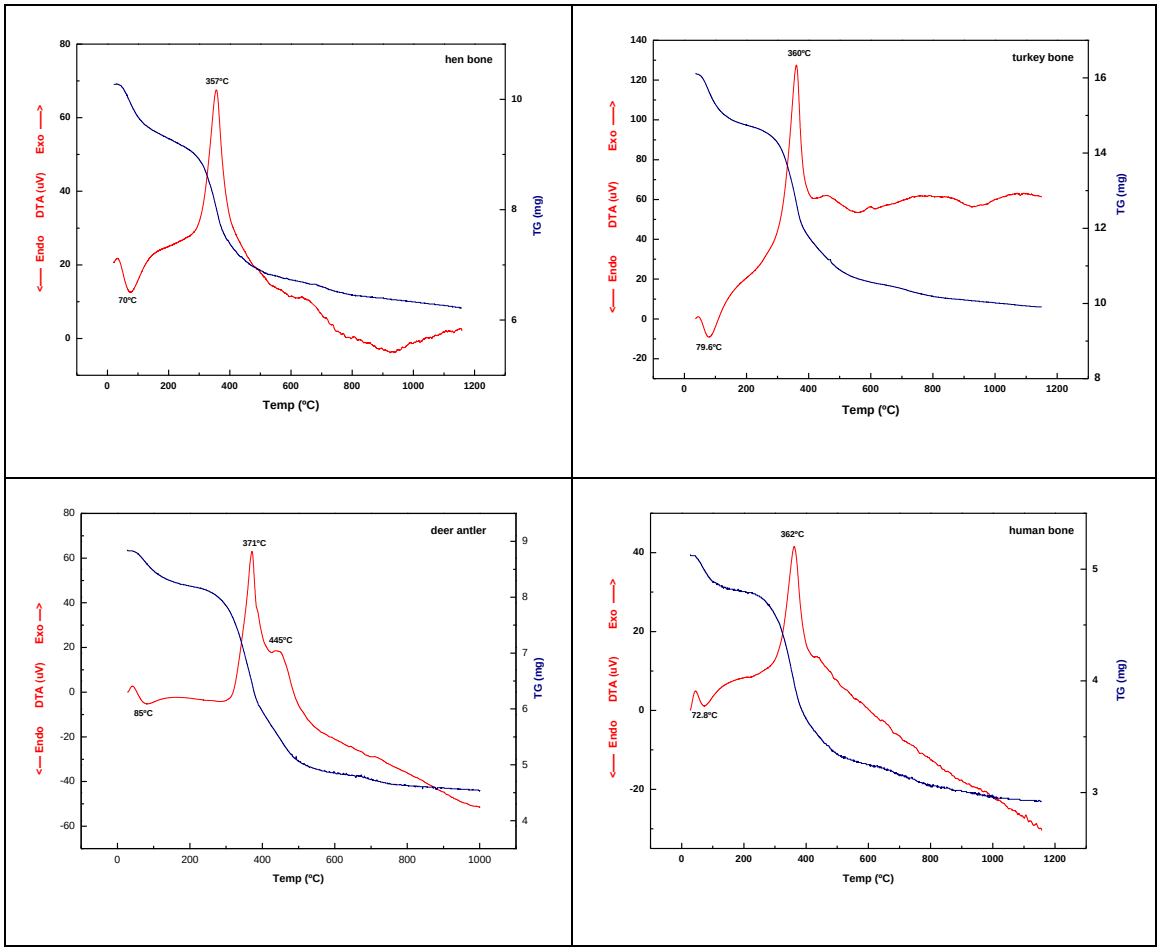

[11] Gelinsky M., Welzel P.B., Simon P., Bernhardt A., König U., Porous three-dimensional scaffolds made of mineralised collagen: Preparation and properties of a biomimetic nanocomposite material for tissue engineering of bone, *Chemical Engineering Journal* 137, 84–96, 2008.

[12] Trębacz H., Wójtowicz K., Thermal stabilization of collagen molecules in bone tissue, *International Journal of Biological Macromolecules*, 37, 257-262, 2005.

[13] Kubisza L., Mielcarekb S., Differential scanning calorimetry and temperature dependence of electric conductivity in studies on denaturation process of bone collagen, *Journal of Non-Crystalline Solids*, 351, 2935-2939, 2005.

[14] Lim J.J., Liboff R., Thermogravimetric Analysis of Dentin, *J Dent Res* , 509-514, 1972.

[15] Chen P.Y., Stokes A.G., McKittrick J., Comparison of the structure and mechanical properties of bovine femur bone and antler of the North American elk (*Cervus elaphus canadensis*), *Acta Biomater*., 5, 693-706, 2009.

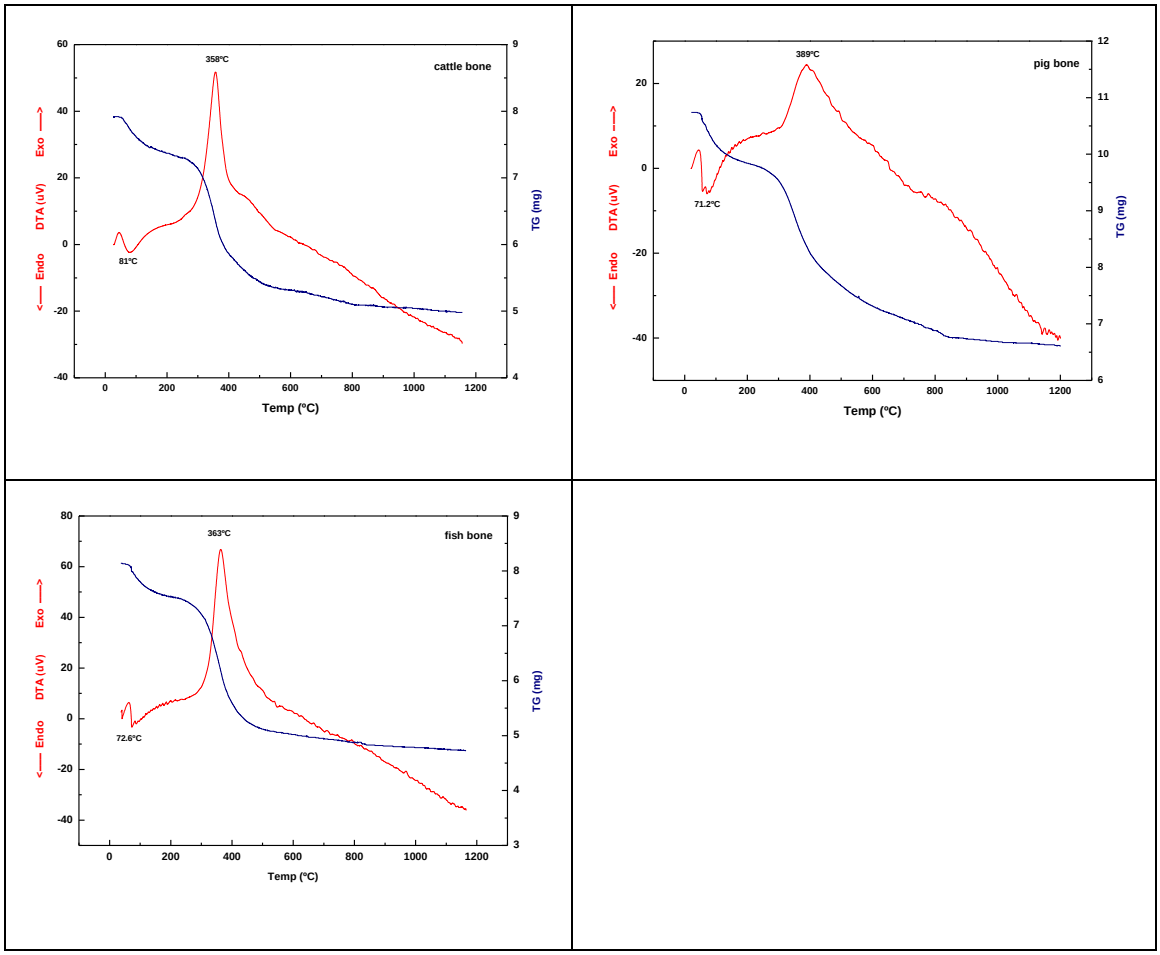

Table 5. *Thermic events and correspondent mass losses determined from DTA /TG analyses*

Sample	Peak I		Mass loss I (%)	Peak II		Mass loss II (%)
	Type	T_{peak} (°C)		Type	T_{peak} (°C)	
Deer antler	Endothermic *collagen denaturation dehydration*	78.9	9.58	Exothermic *decomposition combustion collagen*	401	33.74
Cattle bone		81	7.05		358	24.26
Pig bone		71.2	6.2		389	26.17
Human bone		72.8	5.2		362	30.3
Fish bone		72.6	6.5		363	30.15
Turkey bone		79.6	8.07		360	27.1
Hen bone		70	8.8		357	21

The values of the mass losses accompanying the two thermal events are indicated in *Table 5*. Mass losses for first event are in domain 5.2–9.6%, and those for the second event represent ~20-30% of the material mass, percentages in concordance to the water and organic matter percentages of the total bone tissue mass.

Analyzing these mass losses it can be observed that, considering the water and the organic matter content, *the fish bone* is the material most alike to the *human bone*, having approximatively the same values of the mass losses and also of the maximum temperatures of

each thermic event. The pig bone has about the same water content as the human bone, but the organic proteins content is smaller.

The deer antler presents the highest mass losses values for the both events.

4.3 Kinetic analysis of the reactions thermally activated in deer antler

Preparing a biomaterial of biologic origin for possible applications in bone reconstruction implies, first, the removal of the organic matter in order to avoid antigenic and immunological contaminations. A sterilization process widely used is gamma irradiation. This process offers many advantages which make it attractive as a sterili-zation method in miscellaneous situations in favour of other conventional methods.[16]

Three different ages deer antler samples (3, 4 and 6 years) were subjected to gamma irradiation for 33 hours, with the mean absorption dosis 32,7 ± 1,9 kGy. The nonirradiated samples were labelled according to their age (3, 4 and 6) and the irradiated samples are 3G, 4G and 6G. DSC analyses at three different heating speeds (v_1=3ºC/min; v_2=5ºC/min; v_1=10ºC/min) were performed on the samples 3, 3G, 4G şi 6G.

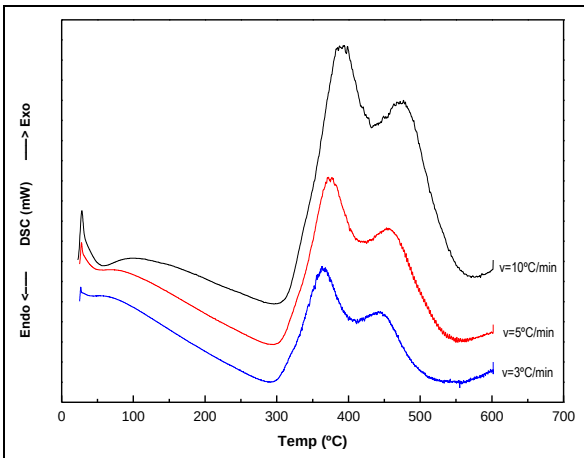

DSC analyses on 3 years non irradiated deer antler

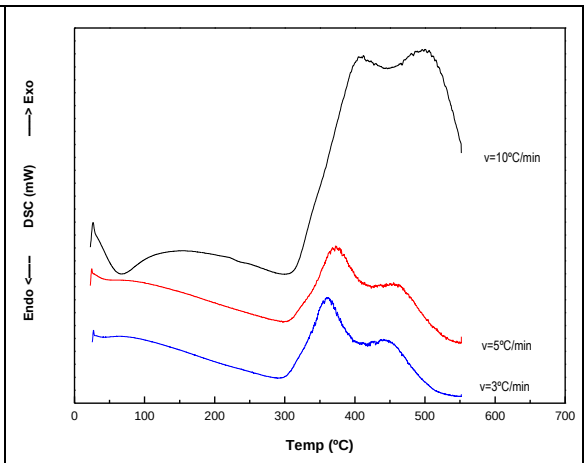

DSC analyses on 3 years γ- irradiated deer antler

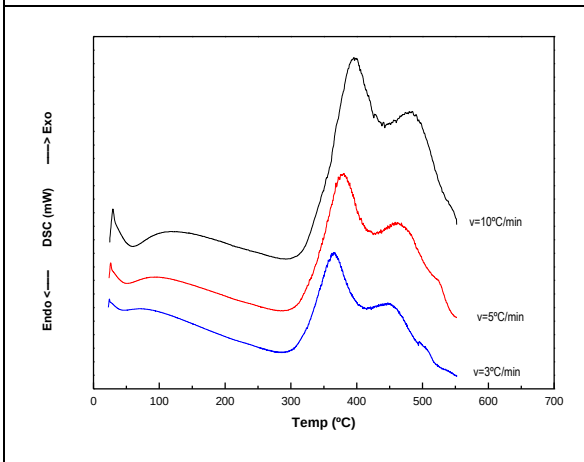

DSC analyses on 4 years γ- irradiated deer antler

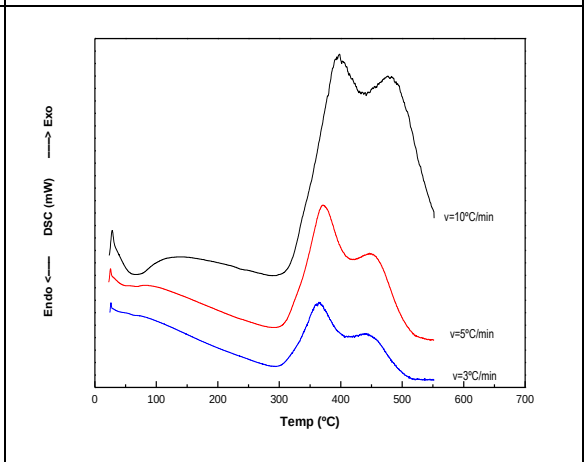

DSC analyses on 6 years γ- irradiated deer antler

[16] Al-Mohizea A.M., El-Bagory I.M., Alsarra I.A., Al-Jenoobi F.I., Bayomi M.A., Effect of gamma radia-tion on the physicochemical properties of ciprofloxacin in solid state, *J. Drug Del. Sci. Tech*., 17, 2007.

In order to determine activation energy of the decomposition reactions of the organic phase in deer antler (E_a) the Kissinger formula was used:

$$\ln(\frac{T_{peak}^{\ 2}}{\beta}) = \frac{E_a}{RT_{peak}} + const.$$

where R is universal gas constant and ß is the heating speed. The E_a se value is obtained from the slope of the plot ln (T_{peak}^2/ß) vs. 1000/T_{peak}. The activation energy values (E_a) calculated from linar fitting of Kissinger equation and peaks corresponding temperatures are presented in Tables 6 and 7. Analyzing these results it can be observed that activation energy has greater values for nonirradiated samples (48.581 kJ/mol the first peak and 60.221 kJ/mol for the second peak) than for gamma irradiated samples (29.823÷34.596 kJ/mol and 38.412÷57.460 kJ/mol). These results can be interpreted on the fact that gamma irradiation affects predominant the collagen matrix by inducing paramagnetic defects[17], which can consist as initiation spots of the decomposition reactions.

Table 6. *Activation energy values calculated from linear representation of ln (T_{peak1}^2/ß) vs. 1000/T_{peak1} for thermic decomposition of the organic phase in the 3 years nonirradiated and 3, 4 and 6 years γ-irradiated deer antler samples*

SAMPLE	**T_{peak1} (ºC)**			**E_{a1} (kJ/mol)**
	Heating speed ß (ºC/min)			
	3	5	10	
3	363.3	371.27	388.54	48.581
3G	361.35	372.42	400.22	29.823
4G	364.33	379.16	400	34.596
6G	364.96	370.02	397.23	34.188

Table 7. *Activation energy values calculated from linear representation of ln (T_{peak2}^2/ß) vs. 1000/T_{peak2} for thermic decomposition of the organic phase in the 3 years nonirradiated and 3, 4 and 6 years γ-irradiated deer antler samples*

SAMPLE	**T_{peak2} (ºC)**			**E_{a2} (kJ/mol)**
	Heating speed ß (ºC/min)			
	3	5	10	
3	443	456	474	60.221
3G	440	455.3	485.79	38.412
4G	451	462	484	57.460
6G	441	448	478	44.872

[17] Băciuț M., Băciuț G., Simon V., Albon C., Coman V., Prodan P., Florian Șt. I., Bran S., Investigation of deer antler as a potential bone regenerating biomaterial, *JOAM*, 9, 2547–2550, 2007.

4.4 Structural analyses of the materials by X-ray diffraction

Systems in study were analyzed by X-ray diffraction on a Shimadzu XRD-6000 diffractometer. The untreated difractograms present apparently a similarity of the structure of the samples, with the presence of a few large peaks specific to crystalline phase of hydroxyapatite [$Ca_5(PO_4)_3OH$].

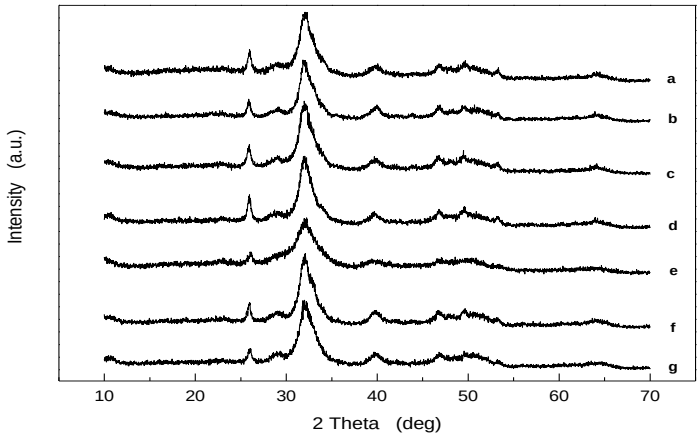

Diffractograms of the untreated sample (a – deer antler; b – human bone; c – pig bone; d – cattle bone; e – fish bone; f – turkey bone; g – hen bone)

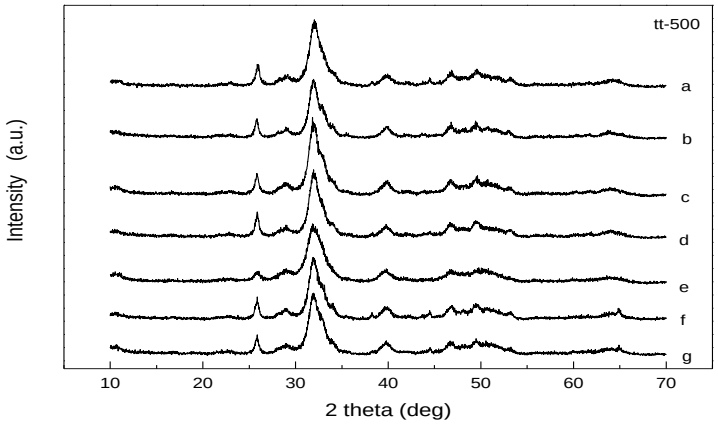

Diffractograms of the thermal treated samples at 500ºC for 2 h (a – deer antler; b – human bone; c – pig bone; d – cattle bone; e – fish bone; f – turkey bone; g – hen bone)

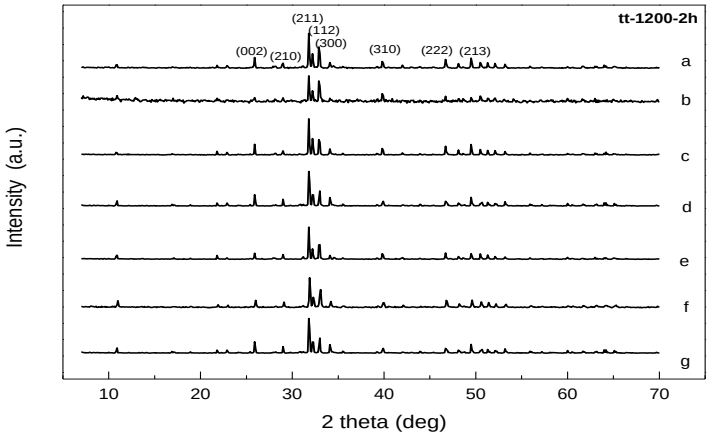

Diffractograms of the thermal treated samples at 1200ºC for 2 h (a – deer antler; b – human bone; c – pig bone; d – cattle bone; e – fish bone; f – turkey bone; g – hen bone)

XRD analyses reveals that the heat treatment at 500ºC for 2 h does not affect the crystalline structure of the samples. It can be discerned but a slightly narrowing of the diffraction peaks, as an effect of the hydroxyapatite crystallites dimensions growth.

On the other hand, the structure of the samples heat treated at 1200ºC for 2 h is significantly affected following this treatment, the anorganic phase in the bones being reorganized by the contribution of the thermal energy in a crystalline structure well defined of pure mineral hydroxyapatite. The medium dimension of the crystallites estimated with the Scherrer equation for the most intense peak is of 14-19 nm.

5. SELECTED CONCLUSIONS

I.

- Aluminosilicate systems with Fe and with radioactivable elements Y and Dy were prepared by sol-gel method: **(100-x)[SiO_2]·20Al_2O_3·x[Fe_2O_3], x = 0, 5, 10, 15, 20% mol**, from TEOS and silicic acid [$Si(OH)_4$] precursors; the systems from silicic acid were prepared with acid and basic pH; **(100-x)[SiO_2]·20Al_2O_3·x[Y_2O_3], x = 5, 10% mol**; **(100-x)[SiO_2]·20Al_2O_3·x[Dy_2O_3], x = 5, 10% mol**, with possible applications in cancer treatments by brachitherapy and hyperthermia.
- Thermal analyses of the samples from TEOS and from silicic acid evidenced that those from silicic acid have a better thermal stability, they present only the mass losses associated to the elimination of the water at the surface, while the samples from TEOS display endothermic peaks associated to decomposition processes and elimination of the nitrates and of the organic monomers remained in the matrix from TEOS precursor.
- The samples were subjected to two heat treatment at 500^oC (30 min) and at 1200^oC (24 h); the samples heat treated at 500^oC presented an amorphous structure; after the heat treatment at 1200 ^oC a crystalline structure appeared and four phases were identified: mullite ($Al_6Si_2O_{13}$), tridimite (SiO_2) (in the systems with no Fe), hematite (Fe_2O_3) and magnetite (Fe_3O_4) in the systems with Fe. The mean dimensions of the Fe oxides crystallites are in the domain of 20-40 nm and they fit the requirements of the hyperthermia practical applications.

II.

- ✓ In the second part of the thesis were analyzed four types of pharmaceutically available mineral clays by methods of XRD, DTA/TG, BET specific surface, porosimetry and SEM in order to found a proper material for advanced applications in cancer treatment by chemotherapy.
- ✓ Structural and thermal analyses revealed the presence of two crystalline phases in each mineral: ALGO → kaolinite – mullite; RN and FAV→ illite – quartz; FARM → kaolinite-montmorillonite – quartz.
- ✓ Specific surface and porosimetry determinations were made on the samples immersed in acid and in basic medium and the results indicate an increase of these properties in ine samples immersed in basic medium.

III.

- ❖ The third part of the work is concentrated on some bone materials with animal and human origin analyzed for application in bone reconstruction purposes.
- ❖ The DTA/TG analyses evidenced two thermic events: first, endothermic, is related to the denaturation of the bone matrix collagen triple helix and to the removal of the water at the

surface of the hydroxyapatite matrix; the second event, exothermic, is associated to the decomposition and the combustionof the organic phase of the bone.

- Structural analyses on the samples not treated and at heat treated samples at 500^{o}C (2 h) and at 1200^{o}C (2 h) indicate that after the heat treatment at 1200^{o}C the structure of the samples become highly crystalline and the hydroxyapatite mineral phase was identified in all samples.
- A kinetic study was conducted on deer antler samples of different ages (3, 4 and 6 years) sterillized by gamma irradiation for 33 hours, the mean absorbtion dosis of 32,7 ± 1,9 kGy. DSC analyses at three heating speeds (v_1=3ºC/min; v_2=5ºC/min; v_1=10ºC/min) were made on samples 3, 3G, 4G and 6G. On the basis of Kissinger equation the plots ($T_{pic}^2/ß$) vs. $1000/T_{pic}$, were represented in order to determine activation energy of the decomposition reactions and of the combustion process in the organic phase of the bone-like deer antler tissue.
- From these results can be observed that activation energy ha highest values for the non irradiated samples and this fact can be explained on the basis that gamma irradiation affects predominantly the collagen matrix by inducing paramagnetic defects which can consist as initiation spots of the decomposition reactions. Moreover, the activation energy of the sample 4G has the highest value therefore this sample might have better mechanic characteristics.

ACKNOWLEDGMENTS

This work was made at the Institute of Interdisciplinary Research in Bio-Nano-Sciences from „Babeş-Bolyai" University in the period 01.10.2006 – 01.10.2010. I would like to express my gratitude and my sincerely thanks to the persons who contribute to my scientific and vocational training.

I express my deepest gratitude to my supervisor, Prof. Dr. Viorica Simon, both in her quality of scientific supervisor and as moral advisor for the completion of this thesis. I thank Prof. Dr. Viorica Simon for offering me excellent guidance and good advices, support and understanding during my research work.

I would like to thank the distinguished reviewers from the Committee: Chairman Prof. dr. Onuc Cozar, Prof. dr. F. Iacomi, Prof. dr. I. Ardelean, Conf. dr. D. Eniu, Prof. Dr. Viorica Simon.

I wish to express many thanks to professors Dr. Simion Simon and Dr. Ioan Barbur for scientific discussions, good advices and sustained encouragements in elaboration of the articles and studies undertaken during my doctoral research period. I express my gratitude for excellent collaboration with persons from other research institutions or faculties: *Prof. dr. Mihaela Băciuț* from „Iuliu Haţieganu" Medicine and Pharmacy University, *Prof. dr. Corina Ionescu* from „Babeş-Bolyai" Univ. Facultaty of Biology Geology and *dr. Cristina Prejmerean* from „Raluca Ripan" Research Institute in Chemistry, Cluj-Napoca.

I am thanking for the help and scientific advices my coleagues from Facultty of Physics and from Institute of Interdisciplinary Research in Bio-Nano-Sciences: dr. Milica Todea, dr. Teodora Radu, dr. Emilia Vanea, Adriana Vulpoi, Horea Mocuța.

I would like also to express my gratitude to my beloved family for their support, understanding, encouragement and love offered me in the period of these 4 years of studies.

Monica Tămăşan

Cluj-Napoca, October 2010